Optically tunable silicon photonic crystal microcavities

Francis C. Ndi, Jean Toulouse

Department of Physics, Lehigh University, 16 Memorial Drive East, Bethlehem, PA 18015
frn2@lehigh.edu

Tim Hodson, Dennis W. Prather

Department of Electrical. & Computer Engineering, University of Delaware, DE 19711

Abstract: We demonstrate the use of silicon photonic crystal based microcavity structures to perform light modulation at potentially giga-Hertz speeds through the use of optically induced plasma dispersion. The cavity configurations considered have the potential to operate at low pump power when the Q of the cavity involved is maximized.

References

1. F. C. Ndi, J. Toulouse, T. Hodson, and D. W. Prather, "All optical switching in Silicon photonic crystal waveguides by use of the plasma dispersion effect," Opt. Lett. **30**, 2254 (2005).
2. R. A. Soref and B. R. Bennett, "Electrooptical effects in Silicon," IEEE J. Quantum Electron. **QE-23**, 123 (1987).
3. J. Vuckovic and Y. Yamamoto, "Photonic crystal microcavities for cavity quantum electrodynamics with a single quantum dot," Appl. Phys. Lett. **82**, 2374 (2003).
4. K. Hennessy, C. Reese, A Badolato, C. F. Wang, A. Imamoglu, P. M. Petroff, E. Hu, G. Jin, S. Shi and D. W. Prather, "Square-lattice photonic crystal microcavities for coupling to single InAs quantum dots," Appl. Phys. Lett. **83**, 3650 (2003).
5. P. R. Villeneuve, D. S. Abrams, S Fan and J. D. Joannopoulos, "Single-mode waveguide microcavity for fast optical switching," Opt. Lett. **21**, 2017 (1996).
6. S. Noda, A. Chutinan and M. Imada, "Trapping and emission of photons by a single defect in a photonic bandgap structure," Nature **407**, 608 (2000).
7. D. W. Prather, J. Murakowski, S. Shi, S. Venkataraman, A. Sharkawy, C. Chen and D. Pustai, "High-efficiency coupling structure for a single-line-defect photonic-crystal waveguide," Opt. Lett. **27**, 1601 (2002).
8. Francis. C. Ndi, unpublished results

1. Introduction

In a previous publication, [1] we demonstrated an all-optical modulation scheme based on the concept of shifting the transmission band-edge of a photonic crystal waveguide. The modulation resulted from a negative change in the refractive index of silicon caused by carriers generated by an optical pump. [2] Although the broadband nature of this scheme is desirable, it becomes pump-inefficient when one wishes to modulate only a single or narrow band of wavelengths. This is because, close to the band-edge, the transmission spectrum of the photonic crystal waveguide is approximately quadratic with wavelength. Consequently, a high pump power is required to cause a large enough shift in the band-edge to achieve a high modulation depth. On the contrary, very high-Q cavity structures with extremely sharp resonances would require comparatively lower pump power to switch from high to low transmission and vice versa. This is primarily because most cavity resonances have a Lorentzian line-shape, with a much steeper drop from the peak of the resonance than the quadratic drop of the photonic crystal waveguide band-edge. The sharper the resonance (or

higher the *Q*), the more sensitive the resonance is to changes in the refractive index and hence the lower the pump power required to modulate the transmission between the peak and shoulder of the resonance.

Extremely high-*Q* photonic crystal based cavity structures have been demonstrated in silicon. [3, 4] In addition, the fact that typical photonic crystal structures are only a few square microns in size means that the area to be illuminated by the pump is also small, leading to increased pump efficiency.

In this paper we demonstrate an all-optical modulation scheme using planar silicon photonic crystal based microcavities. We consider two cavity configurations, the first being a one-dimensional or in-line cavity and the second, a photonic crystal microcavity side-coupled to a photonic crystal waveguide. Some aspects of these cavity configurations have been previously described. [5, 6] Here we provide an experimental demonstration of the usefulness of such structures.

2. One-dimensional cavity

Figure 1 shows the experimental in-line cavity structure considered. The sample was fabricated on a piece of Silicon-On-Insulator wafer using electron beam lithography and reactive ion etching. The wafer had a 0.26μm silicon device layer and a one micron box oxide layer underneath it, as a cladding. The cavity consisted of a section of length *d* of a ridge waveguide, straddled on both sides by two sets of four holes forming the 'mirrors' of the familiar 1D Fabry-Perot etalon. The ridge waveguide had a width of 0.44μm and the holes had a diameter of 0.17μm and a lattice spacing of 0.42μm. The cavity width *d* was 0.57μm.
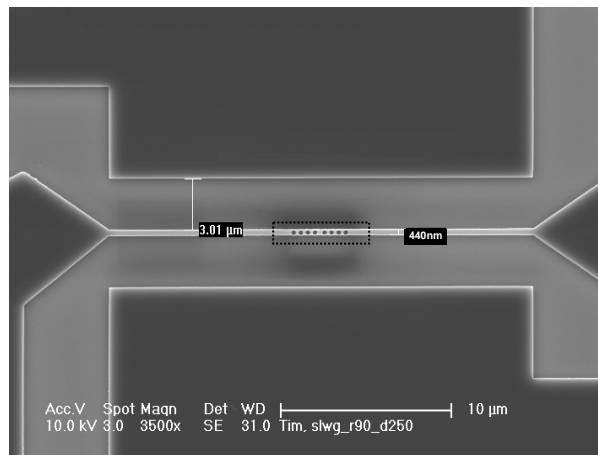

Fig 1. Experimental inline cavity structure

These parameters were chosen iteratively so as to make the resulting structure single mode and to locate the resonance close to the optical communication wavelength of 1550nm. The latter requirement is mainly controlled by the parameter *d*. Light was conveyed to the input and away from the output of the ridge waveguide by planar parabolic reflectors (not fully shown), [7] that served as mode-matching devices between much larger supply guides and the much smaller 1D ridge waveguide.

The characterization set up was the same as that used in Ref. [1]. Figure 2 shows the measured transmission spectra of three experimental samples of increasing cavity length *d*. The peak of the cavity resonance shifts to longer wavelengths with increasing cavity length. This is understandable since for a single-moded 1D cavity, $d = \lambda/2n$, where n and λ are the refractive index of the cavity and the wavelength of interest respectively. Hence, increasing *d* also leads to an increase in the λ transmitted.
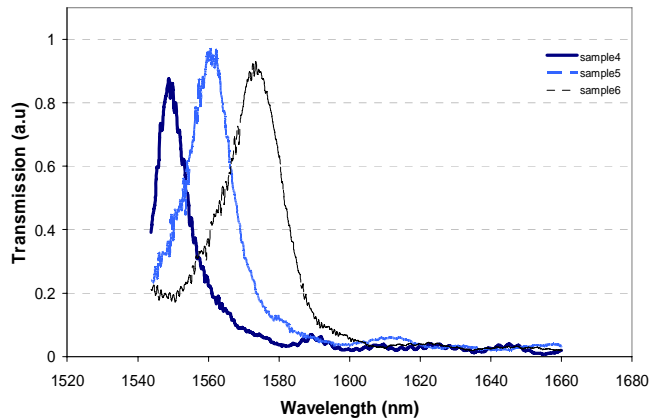
Fig. 2. Measured transmission spectra of experimental sample of inline cavities. The cavity length, *d*, increased from sample4 to sample6.

A second observation from the measured spectra is that the *Q*s of the cavities (defined as $\lambda_o/\Delta\lambda$, were λ_o is the peak resonant wavelength and $\Delta\lambda$ is the width of the resonance) are not very high. In fact, the sample with the smallest width and a peak at 1550nm has a *Q* of approximately 160. It was observed that increasing the reflectivity of the cavity 'mirrors' by increasing the number of holes to five led to a sharp drop in the overall transmission through the structure without a significant increase in the *Q*, suggesting that the *Q*-limiting losses occurred mostly in the direction perpendicular to the direction of propagation. Also, the fact that the sidewall roughness of the samples was less than optimal only worsened the situation. Clearly the benefits of high modulation pump efficiency are not fully realized in this 1D case.

We nevertheless were able to demonstrate transmission modulation using the sample with a peak resonance at 1550nm. The solid curve in Fig. 3 shows the temporal response of the transmission of a probe at 1545nm (left shoulder of resonance) following excitation of the sample by a 30ps pump pulse from a Nd:YAG laser at 532nm (instead of the 3ps Ti:Sapphire pulse used in Ref. [1]). The expectation in this case was that the pump-induced blue shift in the transmission spectrum [1] would lead to an increase in the transmission at this probe wavelength. This expectation is confirmed by the results. The dotted curve in Fig. 3 shows the temporal response of a probe at the peak of the resonance at 1550nm. The expectation in this case was that the pump induced shift would lead to a drop in the transmission at this wavelength, again confirmed by the results. The pump-induced blue shifting of the resonance can be understood by consulting once more the relation $d = \lambda/2n$ for a single-moded cavity of length *d*. The pump causes a reduction of the index n through the plasma effect and, since *d* is fixed, λ must therefore decrease (blue shift) to satisfy this relation.

The measured rise-time of approximately 1ns for both curves in Fig. 3 is most likely limited by the resolution of the 1GHz oscilloscope used in this particular experiment, and the measured relaxation time of approximately 2.5ns is associated with fast carrier removal at the unpassivated silicon surface. The insert in Fig. 3 is the measured response of a photonic crystal waveguide device (of the type discussed in Ref. [1]), following excitation by the Nd:YAG pump pulse (the oscilloscope used in this case had better than 1GHz resolution). The exponential fit to the relaxation part of the response shows a lifetime of 0.67ns, suggesting that such devices can be modulated at GHz speeds. The variation in the response time for different samples is a result of the variation in the surface condition post fabrication. In addition, we have observed that controlled introduction of metallic impurities (gold) can further reduce the response time. [8]

The maximum fractional change in the transmission for both curves in Fig. 3 following excitation by the pump pulse corresponds to an approximate blue shift of 6nm in the

transmission spectrum. This shift is due to a local change of 4×10^{18} cm^{-3} in the carrier concentration or an index change of -0.01. The diameter of the spot size of the pump on the sample was estimated to be 30µm, and using an absorption coefficient of 6.55×10^{3}cm^{-1}, we calculated the pulse energy required to create such a carrier concentration to be approximately 1.6nJ. This value is close to the measured pulse energy of 10nJ if one accounts for losses from beam clipping and reflection. However, we note that the effective area of the sample (denoted by the dotted rectangle in Fig 1) is at least two orders of magnitude smaller than the pump spot size, hence the effective pulse energy required to modulate the transmission is in the range of pico-Joules.
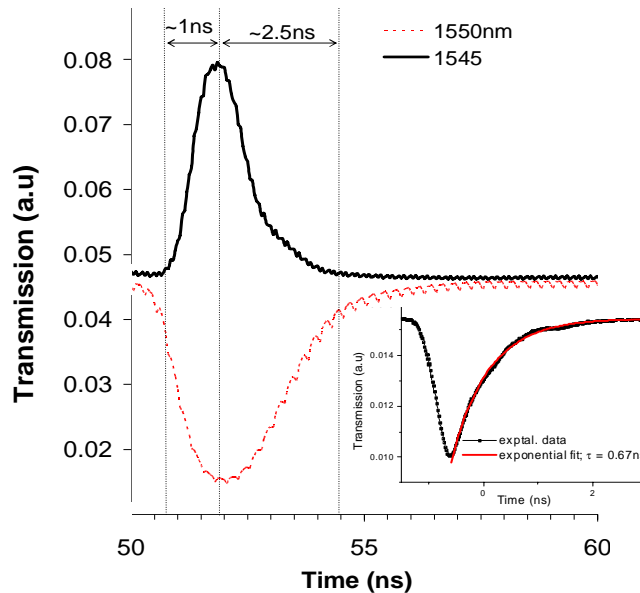
Fig. 3. Temporal response to excitation by a 30ps pulse at 532nm of the transmission of probe light. The probe was first set at 1545nm – solid curve (and then 1550nm – dotted curve), with the expectation that a plasma-induced blue shift in the spectrum would lead to an increase (decrease) in the transmission as observed. The inset shows a sub-nanosecond response of a photonic crystal waveguide to excitation by the Nd:YAG pulse (the rise-time is limited by the bandwidth of the oscilloscope) – demonstrating that GHz modulation speeds are achievable using such devices.

3. Side-coupled cavity

A disadvantage of the in-line cavity configuration is that the photonic crystal mirrors that can potentially provide lossless confinement leading to high cavity Q, is only available in one direction. In this instance, the Q-limiting losses occur along the sides of the waveguide from imperfect index guiding. In an attempt to increase the Q of the cavity while still preserving a relatively high overall transmissivity close to resonance, we considered the cavity configuration shown in Fig. 4. The new sample consisted of a triangular lattice (pitch = 0.42µm) of air holes (diameter = 0.208µm) on a 0.26µm thick symmetric silicon slab. The photonic crystal waveguide was formed by a missing row of nearest-neighbor holes. Sixteen microcavities consisting of enlarged holes (diameter = 0.472µm) were placed symmetrically on both sides of the waveguide along the third row of holes. This configuration was designed to ensure coupling between the guided mode in the waveguide and the mode of the cavities so that at resonance power would leak away from the waveguide into the cavities. The power coupled into the cavities would be lost primarily by out-of-plane scattering because of the lack

of vertical index confinement at the cavities, while the photonic crystal surrounding the cavity provides low-loss confinement in the plane of the lattice.
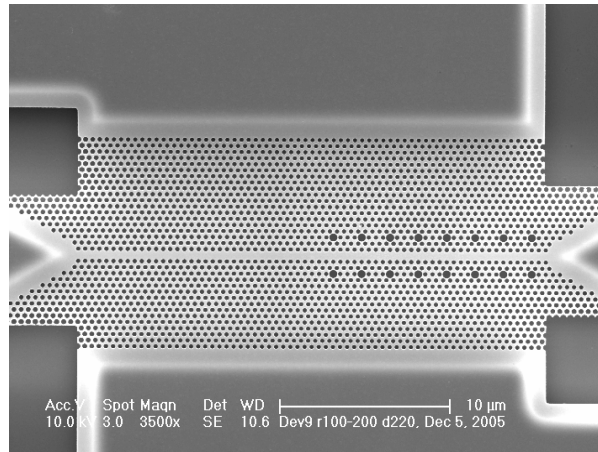

Fig. 4. Side-coupled cavity configuration

The input and output are to the left and right of Fig. 4 respectively. With this configuration the Q of the cavities can be optimized without impeding the overall transmission though the structure.

Figure 5 shows the measured transmission spectrum of the sample with a drop in the transmission at the resonant wavelength of 1563nm.
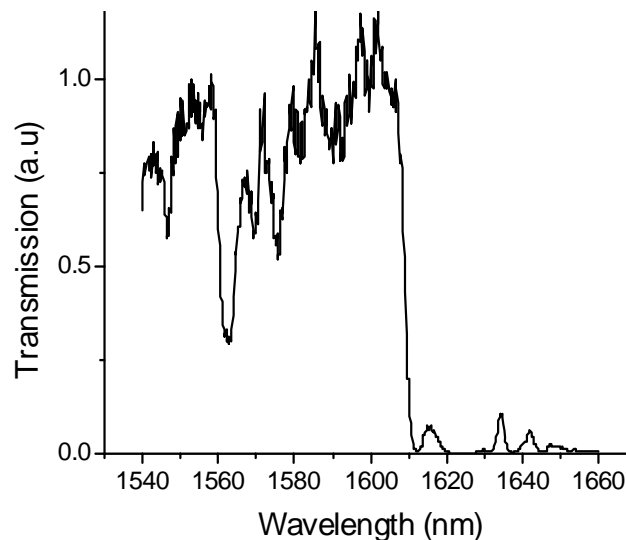

Fig. 5. Transmission spectrum of side coupled cavity showing a resonance at 1563nm

The percentage of power lost to the cavity is dependent on the relationship between the in-plane and out-of-plane Qs of the cavity, with up to a 50% transfer when the two Qs are equal. [6] In this case we use a greater number of cavities to guarantee that the cumulative loss is significant and can be added as needed to completely eliminate the resonant wavelength from the output, although, fabrication imperfections may result in the different cavities having

slightly different resonant wavelengths when the cavity Q is very high. However, the measured Q in this instance is only 270 so that this is not a relevant problem (the other smaller dips in the spectrum are mostly a result of non-uniform coupling at the input of the waveguide).

Figure 6(a) is a picture taken by a near infra-red camera, showing high transmission at a non-resonant wavelength, indicated by the scattered light at the input (bottom) and output (top) of the photonic crystal waveguide. At the resonant wavelength (1563nm), Fig. 6(b) shows that the light couples to and is scattered out-of-plane by the cavities.

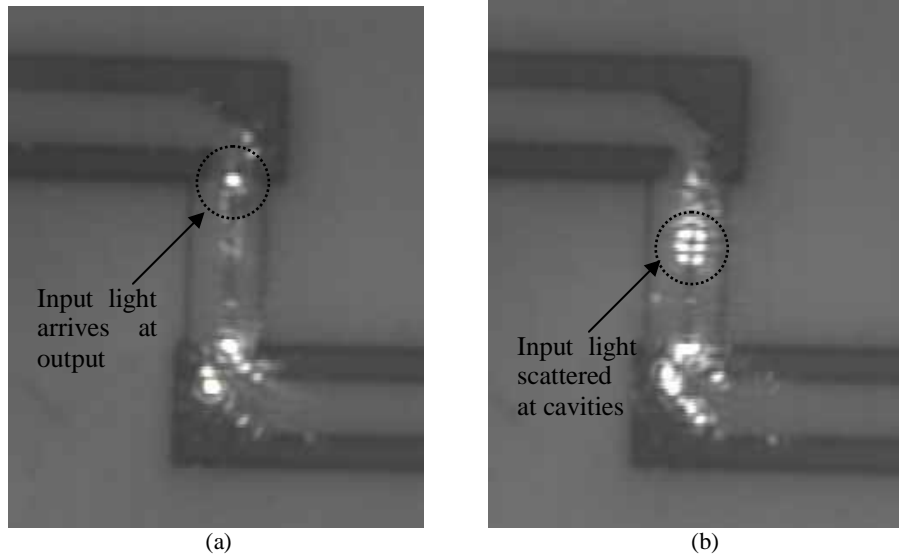(a)   (b)

Fig. 6. (a) High transmission at a non-resonant wavelength, illustrated by the scattered light at the input and output of waveguide. (b) At the resonant wavelength most of the light couples to the cavities and is scattered out-of-plane.
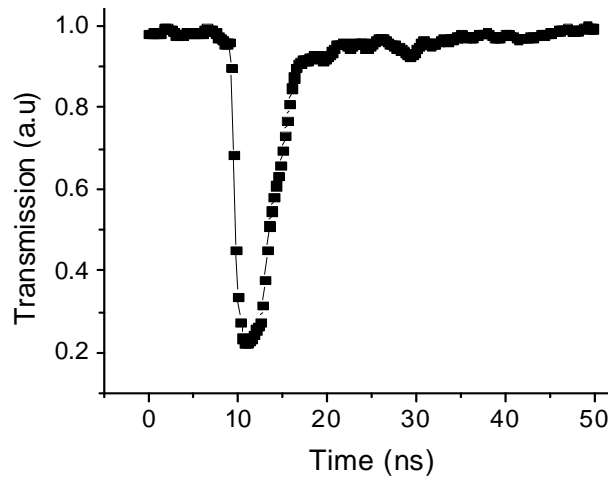

Fig. 7. Transmission modulation near resonance using a 30ps optical pump pulse at 532nm.

Figure 7 shows the temporal response of the transmission of a probe at 1559nm (shoulder of resonance) following excitation of the sample by a 30ps optical pump pulse from a Nd:YAG laser at 532nm. The blue shift in the transmission spectrum causes a drop in the transmission at this wavelength, as expected, with a response less than 5ns.

4. Summary

We have experimentally demonstrated the use of photonic crystal micro-cavity structures (both in-line and side coupled to a photonic crystal waveguide) to perform transmission modulation. These configurations have the potential to operate at low pump power when the Q of the cavities involved is maximized or, in other words, when the resonance of the cavities is very sharp. Although not fully realized here due to fabrication imperfections, other authors have demonstrated compact silicon photonic crystal based micro-cavities with extremely high Qs. Combined with the modulation scheme presented in this work, such high-Q cavity structures have the potential to achieve very compact, highly power-efficient modulators that can be integrated with other components on a silicon substrate.